A&A 401, 699–709 (2003)
DOI: 10.1051/0004-6361:20030089

Astronomy & Astrophysics

A self-consistent treatment of radiation in coronal loop modelling

S. J. Bradshaw and H. E. Mason

Department of Applied Mathematics and Theoretical Physics, Centre for Mathematical Sciences, University of Cambridge, Wilberforce Road, Cambridge, CB3 0WA, UK

Received 11 November 2002 / Accepted 21 January 2003

Abstract. We perform a hydrodynamic simulation of a cooling coronal loop and calculate the time-dependent ion populations of the most abundant elements of the solar atmosphere at each time-step. We couple the time-dependent ion balance equations to the hydrodynamic equations in order to treat the energy loss through radiation in a self-consistent way by allowing for the emission from a potentially nonequilibrium ion population.

We present results for the response to the changing conditions in the loop of the population of C VII ions and find significant deviations from equilibrium in the coronal and footpoint regions of the loop. The former is due to the tenuous nature of the coronal plasma causing recombinations to be rare and the latter is due to the strong downflows that develop as the loop cools, which carry persistent C VII ions into the lower regions of the loop. We also present a comparison between total plasma emissivity curves calculated during this simulation and an almost identical simulation that assumed an equilibrium ion population for the calculation of the radiation term. As a result of the nonequilibrium ion populations we find significant differences between the emissivity curves of each simulation and the loop cooling times.

We suggest that a consideration of nonequilibrium ionisation and radiation might help to (a) explain the thermal broadening observed in some emission lines during explosive events, and (b) reconcile differences between theory and observations relating to the longevity of some loops observed in the TRACE filters.

Key words. Sun: corona

1. Introduction

The current generation of solar missions have revealed a wealth of structure comprising the solar corona in terms of magnetic loops configured in myriad ways, giving rise to the many and varied phenomena observed. The dramatically improved temporal cadence of modern observing instruments has also revealed a wealth of dynamical activity. Indeed, the long-standing problem in modern astrophysics of how the corona is heated to temperatures several orders of magnitude above the solar surface temperature is now a matter of ascertaining not only the spatial dependence, but also the temporal dependence of the potential heating mechanisms that are able to reproduce the temperature, density and velocity profiles measured in coronal loops.

In order to address this problem a large amount of effort in theoretical work has been put into developing models of coronal loops. These models fall into two broad classes: static models and dynamic models. The work of Priest et al. (1998) has shown that the footpoint to apex temperature profile calculated under the assumption of static conditions within a loop is highly sensitive to the spatial distribution of heat deposition along it. It is a relatively straightforward matter to calculate static solutions to the system of hydrodynamic equations with a functional form for the heat input and many authors have followed this line of reasoning.

Aschwanden et al. (2001) have made observations of many loops using the TRACE satellite and analysed the data using filter ratio techniques. Their comparison of observed temperature profiles, shown to be approximately isothermal, with temperature profiles calculated using a static model led to the conclusion of a predominance of heat input towards loop footpoints and therefore one must look to mechanisms capable of depositing heat in these regions. However, Schmelz et al. (2001) undertook a different kind of analysis using a technique relying upon the differential emission measure of the loop plasma and showed the loops they observed to be multi thermal in the magnetic field direction. In this case one is led to the conclusion of a more spatially uniform deposition of heat.

There are several variations on this theme, for example Reale & Peres (2000) have suggested that observations can be theoretically reproduced by modelling loops as a bundle of filamentary threads. Each thread is heated uniformly and there is a statistical distribution of peak temperatures among the threads. They argue that such a bundle, when observed by TRACE and using filter ratio techniques to analyse the data, would be

Send offprint requests to: S. J. Bradshaw,
e-mail: S.J.Bradshaw@damtp.cam.ac.uk

interpreted as an isothermal loop structure in the limit of the spatial resolution of the instrument.

Others have argued that the observed presence of strong flows within many loops invalidates the static assumption and in this case one must look to the considerably more complicated case of hydrodynamic modelling, in which flows, waves and even shocks must be accounted for. Clearly, the active heating mechanism(s) must be able to explain all of the observed phenomena and therefore many authors have argued that the physics of coronal loops can only be understood through hydrodynamic modelling with a form for the heating that varies in time as well as spatially.

Parker (1988) has suggested that the corona is heated to X-ray temperatures by a swarm of nanoflares, small-scale magnetic reconnection events that release heat into the corona and are driven by the braiding of magnetic field lines due to convective motions in the photosphere. Mendoza-Briceño et al. (2002) have calculated the response of coronal plasma to observed transition region activity (explosive events, microflares, blinkers, etc.) and have found results in terms of the temperature profile in qualitative agreement with those of Aschwanden et al. discussed above. Teriaca et al. (1999) have investigated the observed red-shift of mid-low transition region lines and the blue-shift observed in low coronal lines, and conclude that the occurence of a nanoflare at the O VI formation temperature might plausibly account for the measured velocity profiles. Warren et al. (2002) have performed hydrodynamic simulations of a bundle of loops impulsively heated in their transition regions, which are then allowed to cool through temperatures corresponding to the TRACE 171 Å (Fe IX/X) and 195 Å (Fe XII) bandpasses. They find that such a bundle of loops would have an isothermal filter ratio temperature when observed with TRACE.

In most cases it is determining the form of the heating function that has been given priority and has proven the main source of contention among authors. This has been partly due to a lack of consistency between observations and also due to a number of competing heating mechanisms favoured by different authors.

Cargill et al. (1995) point out that the temporal evolution of the temperature and density in a cooling postflare loop is also sensitive to the details of the radiative loss function. In the hydrodynamic equations the heating and the radiation are described by source and sink terms respectively. Therefore, it is evident that if the temperature profile of a loop is sensitive to the deposition of energy (heating) then it must also be sensitive to the removal of energy (radiation). A lack of a thorough treatment of radiation in theoretical modelling may well lead to ambiguous conclusions about the nature of coronal heating. If one considers a time-dependent deposition of heat into the corona then one must also consider the time-dependent response of the corona, not only through flows and conduction, but also through radiation. In general, hydrodynamic modelling has been performed with a time-dependent heating function and yet radiation is calculated assuming equilibrium conditions.

In the present paper we address this inconsistency and perform a hydrodynamic simulation with a time-dependent radiation function, thereby allowing radiation away from conditions of equilibrium. We simulate a loop as it cools from a peak temperature of approximately 1.5 MK and calculate the ion populations of the fifteen most abundant elements in the solar atmosphere, as prescribed by Feldman (1992). We make no attempt in the present paper to compare our results with a set of observations. Our intention is to perform a theoretical simulation of a physically reasonable loop and to highlight the importance of considering radiation away from conditions of equilibrium.

2. Hydrodynamic modelling

The details of the hydrodynamic code developed for the purposes of the current study, the numerical methods and comparisons with the results of independent codes are left to a subsequent paper. However, good qualitative agreement during tests has been found with the transient heating simulations of Spadaro et al. (2002) and the explosive event modelling of Sarro et al. (1999), under the assumption of ionisation equilibrium radiation. There are, to the best of the authors' knowledge, no published results of simulations of solar or stellar atmospheres that have been performed with a fully self-consistent hydrodynamic and time-dependent radiation code.

We solve the one-dimensional form of the hydrodynamic equations in the static equilibrium limit in order to derive our initial ($t = 0$) loop atmosphere. This initial hydrostatic solution is obtained by integrating the energy and the pressure equations from the loop footpoint to its apex to derive the temperature and pressure profiles. These profiles are then mirrored about the loop apex under the assumption of apex symmetry to derive the footpoint to footpoint profiles required by the hydrodynamic code. We do not allow the temperature in the static equilibrium solution to vary by more than 5% in a single spatial step and therefore this requirement determines the resolution of the fixed, non-uniform grid used to perform the hydrodynamic simulations. In the transition region we achieve a resolution on the order of 100 metres and in the corona the grid resolution is on the order of 100 kilometres. We also limit the variation in width of adjacent cells in order to avoid the well-known problems that may arise due to a loss of order in calculating spatial derivatives if this is not accounted for (Oran & Boris 2001).

For boundary conditions we choose a footpoint temperature of 20 000 K and set the conductive flux to zero. This represents a physically reasonable lower boundary condition in the absence of a detailed knowledge and thorough treatment of the deep chromosphere and photosphere (Klimchuk 2002, private communication). The simplest case of uniform heat deposition along the loop is assumed and the loop reaches a peak temperature at its apex of approximately 1.5 MK. By symmetry, the conductive flux also disappears at the apex.

When the initial static equilibrium atmosphere has been calculated the characteristic variables of temperature and pressure, defined at the cell edges, are converted into the conserved variables of mass density, momentum density (zero at $t = 0$) and internal energy density, which are then interpolated back onto the fixed, non-uniform grid in the cell centres. As a result of this process there is no longer a perfect balance of the

forces and energy fluxes. Therefore, we adopt the approach of Klimchuk et al. (1987) by treating these imperfections as small amplitude perturbations and allowing them to evolve. For the case considered in the current paper they quickly become swamped by large scale downflows developing as a result of the radiative cooling and consequently have no effect upon the evolution of the plasma.

We solve the conservative form of the hydrodynamic equations as generally recommended for numerical work:

$$\frac{\partial \rho}{\partial t} + \frac{\partial}{\partial s}(\rho v) = 0, \tag{1}$$

$$\frac{\partial}{\partial t}(\rho v) + \frac{\partial}{\partial s}\left(\rho v^2\right) = \rho g_{\parallel} - \frac{\partial P}{\partial s}, \tag{2}$$

$$\frac{\partial E}{\partial t} + \frac{\partial}{\partial s}\left[(E+P)\,v\right] = \rho v g_{\parallel} + \frac{\partial}{\partial s}\left(\kappa T^{5/2}\frac{\partial T}{\partial s}\right) + E_{\rm H}(s,t) - E_{\rm R}(s,t), \tag{3}$$

$$E = \frac{1}{2}\rho v^2 + \frac{3}{2}k_{\rm B} n T, \tag{4}$$

$$P = 2k_{\rm B} n T. \tag{5}$$

Here ρ, v, P and T are the mass density, bulk velocity, total pressure and temperature, respectively; $g_{\parallel}$ is the gravitational acceleration parallel to the magnetic field; $k_{\rm B}$ is the Boltzman constant; κ is the coefficient of thermal conductivity; $E_{\rm H}$ is the volumetric heating rate; and $E_{\rm R}$ is the energy loss rate due to radiation. Note that $E_{\rm R}$ is now a function of s and t and accounts for departures from ionisation equilibrium of the population of emitting ions.

In common with Mendoza-Briceño et al. (2002) and Spadaro et al. (2002) we impose rigid wall, fixed value boundary conditions at the chromospheric footpoints. Since we are simulating a cooling loop and the footpoints are sufficiently deep in the atmosphere these boundary conditions have no effect upon the evolution of the coronal plasma. Also, in common with other authors (Spadaro et al. 2002; Klimchuk et al. 1987), we smoothly decrease the radiation to zero in regions where the temperature begins to approach the footpoint temperature of 20 000 K. This somewhat artificial device helps to avoid a problematical radiative instability developing at the loop footpoints, due to the n^2 dependence of radiation, inherent in loop modelling.

To accurately calculate the transport terms of the hydrodynamic equations we use Barton's method for monotonic transport and a staggered leapfrog algorithm to perform the time integration. Centrella & Wilson (1984) provide a detailed discussion of Barton's method, which is a simpler and more rugged version of the method devised by van Leer (1977), and which works well even on highly discontinuous hydrodynamic problems. The conductive flux (diffusion) term is solved using an explicit method, which is more accurate than implicit methods provided one has sufficient computational resources to perform the calculation for the small time-steps that can be necessary to satisfy the stability condition. All other ordinary and source/sink terms are time integrated using standard Runge-Kutta methods (Press et al. 1995).

To perform the simulation we begin with our initial loop atmosphere and solve the hydrodynamic equations as described above, allowing our initial atmosphere to cool by switching off the background (uniform) heating term.

3. Nonequilibrium ion populations

In equilibrium, it is assumed that the ion populations respond instantaneously to changes in the plasma temperature. For example, in a plasma at an equilibrium temperature of 1.5 MK one would expect carbon to be almost entirely in the form of C VII (fully ionised carbon), see Arnaud et al. (1985) and Mazzotta et al. (1998). However, if there is an extremely rapid change in temperature, such as might occur when a very large amount of heat is deposited very quickly, then the assumption that the ion populations respond instantaneously is invalid and ions of relatively low charge can potentially exist at much higher temperatures than usual. The ion populations are said to be shifted out of equilibrium. The same is true of a rapidly cooling plasma, in which case ions of high charge states can exist at much lower temperatures than they would otherwise be found. The implications for observational data analysis are extremely significant, as one might easily draw erroneous conclusions about the plasma temperature from a consideration of the ion populations alone.

A number of authors have investigated the response of the ion populations of particular elements to a strong heating event. MacNeice et al. (1984) calculated the departure from equilibrium of the population of calcium ions during a solar flare and Erdélyi et al. (1998), Erdélyi & Sarro (1999) and Sarro et al. (1999) investigated the departure of the C IV ion from its equilibrium population during explosive events localised in the transition region.

MacNeice et al. calculated shifts in the peak ion abundance temperatures of about 10% between time-dependent and steady-state ion populations. They concluded the radiated power, taking account of time-dependent ionisation, was therefore only about 5% greater than the steady-state power loss assumed in their calculations. However, their calculations were performed at very large electron number densities ($n > 10^{12}$ cm^{-3}) with correspondingly frequent ionisations and recombinations. Sarro et al. found that the thermal widths of the carbon lines they calculated were larger than would be expected if the lines were formed at their equilibrium temperature, a natural consequence of the fact that excitation and radiative decay occurs on shorter time-scales than ionisation and recombination, and that ions generally radiate more strongly at temperatures above their formation temperature.

In both cases, despite attempting to calculate the departure from equilibrium of an ion population, the authors used a radiative loss function calculated under the assumption of an ion population in equilibrium. This represents an inconsistency, although in the case of MacNeice et al. it is probably a reasonable approximation due to the high densities involved. However, in the case of a rarefied plasma such as the corona it is an extremely important consideration, because the characteristic lifetime of an ion population in such a tenuous plasma can easily be on the order of (and even greater than) the

characteristic time-scale of the temperature changes due to cooling and heating events (see Sect. 4). Since it is the ions that are radiating, and their energy level excitation and decay time-scales are much smaller than their lifetimes, the amount of energy radiated when the ion populations are shifted away from equilibrium must be used for the sink (radiation) term of the hydrodynamic equations in order to perform a fully self-consistent calculation. This requires a coupling between the hydrodynamic equations and the system of detailed ionisation balance equations (one for each ion of every element considered).

We demonstrate the importance of this effect by solving the detailed ionisation balance equation for each ion of the fifteen most abundant elements of the solar atmosphere during a hydrodynamic simulation of a cooling loop:

$$\frac{\partial Y_i}{\partial t} + \frac{\partial}{\partial s}(Y_i v) = n\left(I_{i-1}Y_{i-1} + R_i Y_{i+1} - I_i Y_i - R_{i-1}Y_i\right). \qquad (6)$$

Y_i denotes the fractional population (normalised to 1) of ion stage i of element Y; the coefficients I_i and R_i are the ionisation and recombination rates from/to ion stage i in units of cm^3 s^{-1}; n is the electron number density (cm^{-3}); t is time (s); and the spatial location along the loop is denoted by the curvilinear coordinate, s (cm).

The newly calculated ion populations are then used in the calculation of the radiation term at each time-step, thus providing the necessary coupling between the systems of equations. We assume that the fifteen most abundant elements are sufficient by themselves to provide a physically reasonable and accurate calculation of the total radiative energy loss from the entire loop. The other values required in order to complete the radiation calculation are:

(a) The sum total of the line intensities emitted by each ion. These are calculated by interpolation on a grid of values (as a function of density and temperature) provided by the CHIANTI atomic database (Dere et al. 1997; Young et al. 2003).

(b) A set of elemental abundances. The abundances of Feldman (1992) (with a high coronal metallicity) are used in the present work. As a caveat to this, Widing & Feldman (2001) have shown that the elemental composition of active regions can also change over time. Therefore, one cannot necessarily assume a steady-state elemental abundance when modelling.

(c) A set of ionisation and recombination rates. We adopt the rates due to Mazzotta et al. (1998) calculated in the low electron density limit. In future work it will be necessary to consider the density dependence of, for example, dielectronic recombination and also charge transfer reactions, when attempting to model the deeper layers (e.g. the chromosphere and photosphere) of the solar atmosphere where the plasma can no longer be assumed optically thin.

In the present work the low density, optically thin assumption is reasonable because we are mainly interested in the coronal ion populations and the range of densities encountered during the simulations is only 10^7–10^{10} cm^{-3}.

4. Discussion of theoretical results

Figure 1 shows a time series of footpoint to footpoint temperature profiles taken at representative intervals in time to demonstrate how the simulated loop cools from a peak temperature of about 1.5 MK, to a peak temperature of about 0.3 MK, during a period of 1500 s. Again, we emphasise that our intention is not to provide a simulation of a cooling loop to be compared with observations, but to investigate the departure from equilibrium of an ion population in the rarefied plasma of the corona while treating the radiation in a self-consistent way, during a process taking place under physically reasonable conditions and time-scales.

An identical simulation, with the same initial conditions, was carried out using a radiative loss term calculated assuming equilibrium for the purposes of comparison. We found that the equilibrium simulation reached its termination condition ($T \sim 10^4$ K) significantly faster (about 10 min) than the nonequilibrium simulation. This result might well have important ramifications for the simulation of cooling loops if the assumption of equilibrium radiation tends to cool the loops too quickly. It is especially interesting to consider what might happen to a very hot loop as it cools through the TRACE filters under these circumstances (Erdélyi & De Pontieu 2002, private communication). We discuss this more fully in Sect. 5.

Figure 2 shows a time series of C VII population profiles taken at the same times as the temperature profiles of Fig. 1. The ion populations are normalised to 1. For example, Fig. 2 shows that at $t = 0$ about 70% of carbon is present in the form of C VII at the loop apex ($s = 4 \times 10^9$ cm) and no carbon is present in the form of C VII at the loop footpoints.

We confirm this by examining Fig. 3, which is an equilibrium ionisation balance for carbon, calculated using the ionisation and recombination rates of Mazzotta et al. (1998). At $t = 0$ our loop has an apex temperature of about 1.5 MK and Fig. 3 shows that approximately 70% of carbon present should be in the form of C VII. This is exactly as expected since our initial ($t = 0$) conditions are calculated in equilibrium.

During the first minute of the cooling simulation the loop cools to an apex temperature of about 1.35 MK and there is no appreciable change in the population of C VII in Fig. 2. However, the steep gradient in the 1 MK region of the C VII equilibrium population suggests that there should have been a significant change in the C VII population. Therefore, the population of C VII is shifted away from equilibrium very quickly indeed. This also means that there is much less C VI than would be expected in an equilibrium population at the same temperature.

After 300 s the loop top temperature is about 0.9 MK and the departure from equilibrium of the population of C VII is even more pronounced, since according to Fig. 3 C VII should almost have disappeared in equilibrium conditions.

In order to check our hydrodynamic calculations we may determine the characteristic lifetime of the ion: since C VII is fully ionised carbon we consider only the recombination rate and estimate the lifetime of the ion in a plasma of a given temperature and density. Following Mazzotta et al., the recombination rate corresponding to C VII at a temperature of 1 MK is

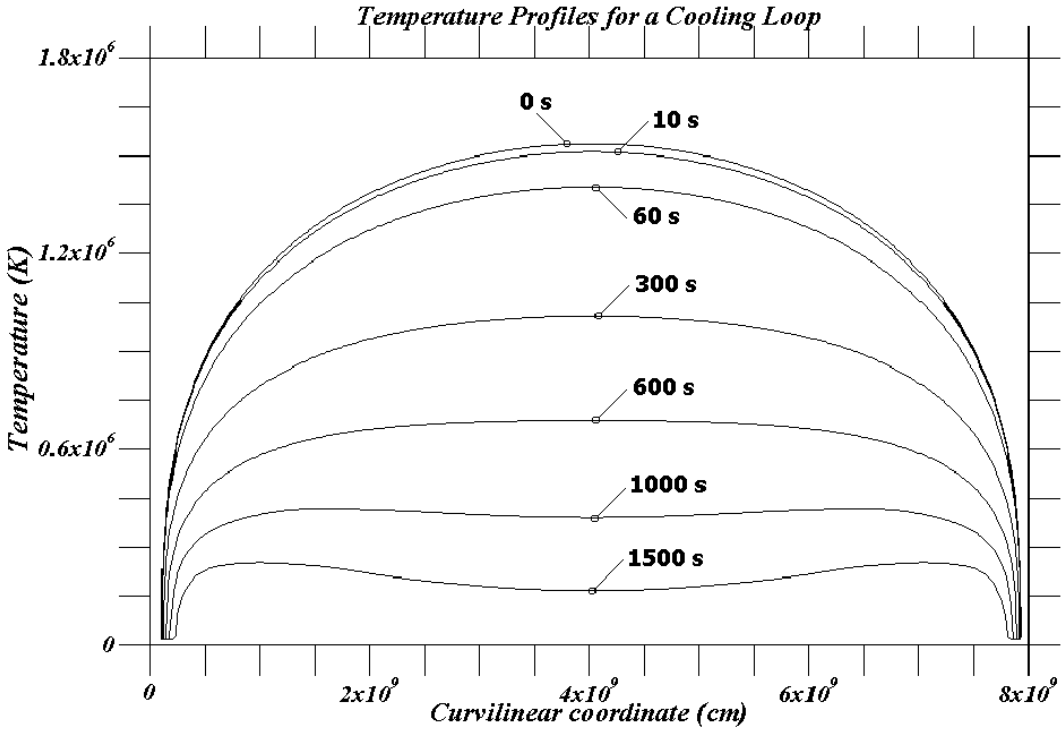

Fig. 1. A time series of temperature profiles of the cooling loop.

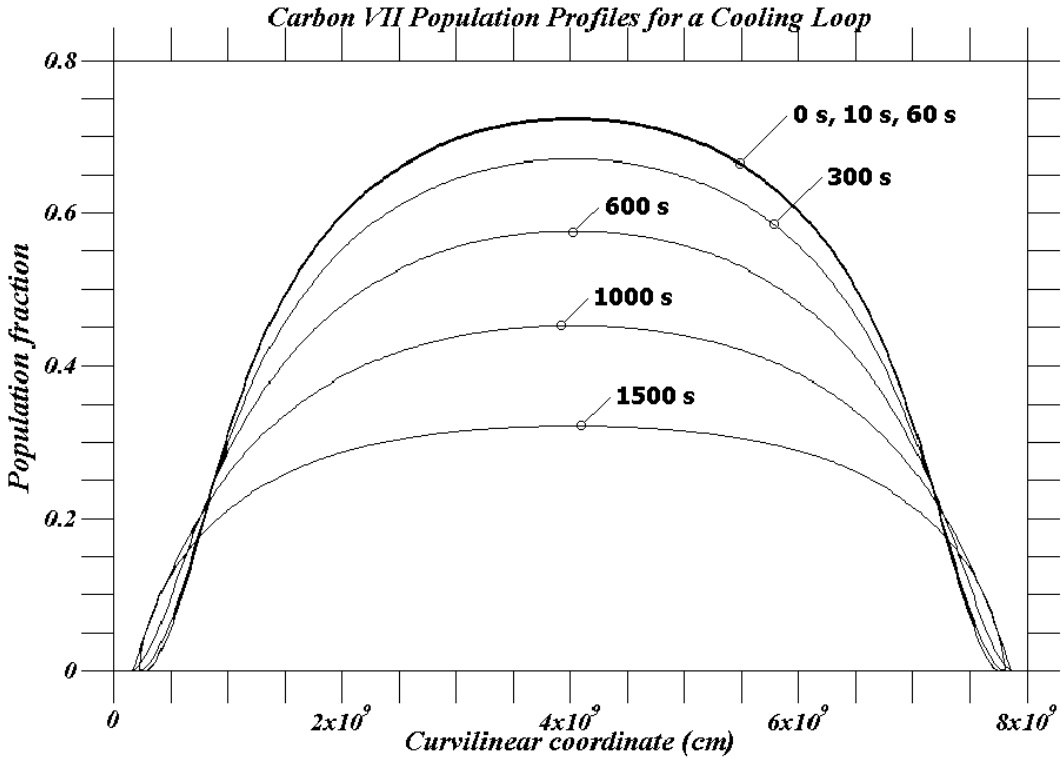

Fig. 2. A time series of C VII profiles for the cooling loop.

1.1840×10^{-12} cm^3 s^{-1}. We now require the number density to complete the calculation. As the loop radiates strongly from its dense footpoints, due to the n^2 dependence of radiation, downflows develop in order to try to balance the energy loss (Fig. 4). However, during the first 300 s of the simulation the downflows are not too strong and the coronal density does not change significantly because very little coronal material is carried away. Therefore, we may take the electron number density of our initial atmosphere, which is about 4×10^8 cm^{-3} throughout most of the coronal region. We estimate the characteristic lifetime

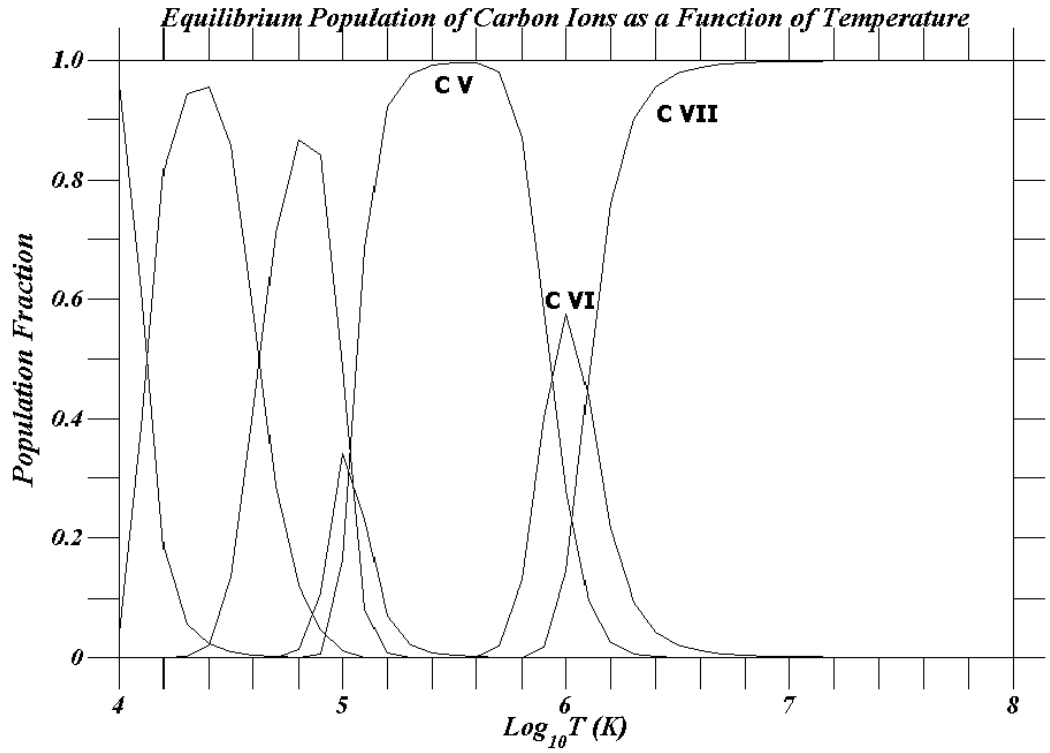

Fig. 3. Carbon equilibrium ionisation balance.

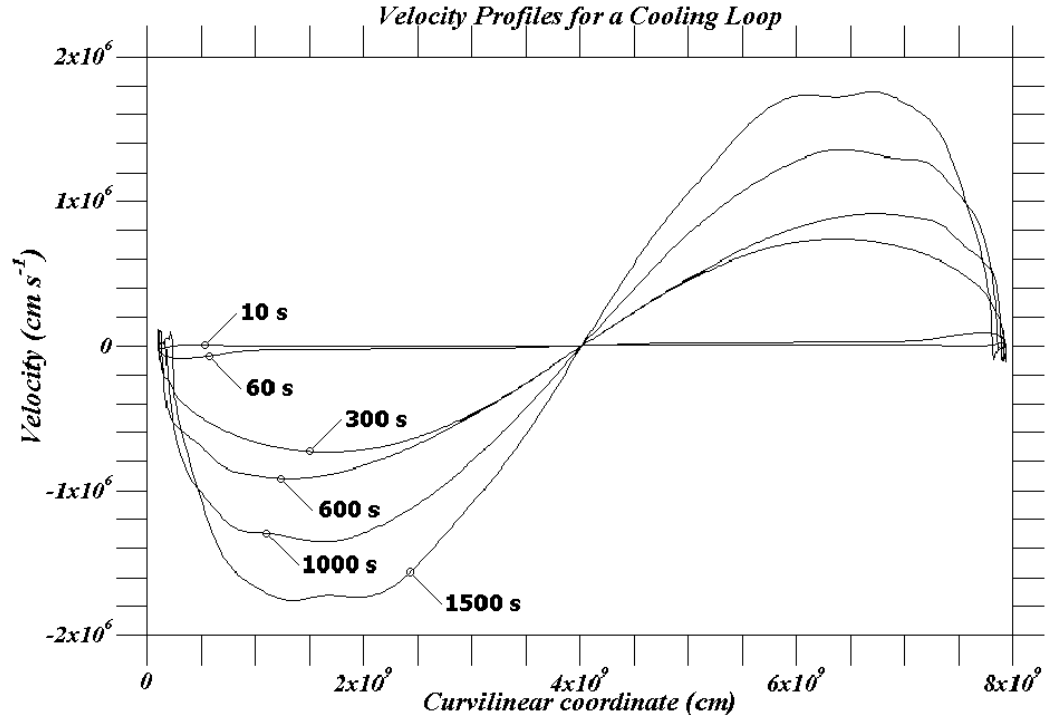

Fig. 4. A time series of velocity profiles along the cooling loop. The velocity is taken positive when the plasma motion is in the direction of increasing curvilinear coordinate.

of C VII in the coronal region of the loop, at the specified temperature and density, during the first 300 s of the simulation to be about 2000 s.

Therefore, we may expect C VII to persist for time-scales on the order of 2000 s under the conditions in the simulated loop. Our calculation is clearly consistent with this estimate because C VII has not disappeared after 300 s, as the equilibrium ion population suggests that it should have done, and remains the most abundant of the carbon ions.

As the temperature decreases the recombination rate of C VII increases. However, as the downflows grow stronger and material is carried away from the coronal region the density

will decrease. Consequently, the characteristic lifetime of C VII remains appreciable and this is clearly shown in Fig. 2 by the fact that even after 1500 s C VII still represents a significant fraction of the coronal abundance of carbon. In fact, had the coronal density remained constant then we would still expect a non-negligible amount of C VII to remain in the corona because of the length of its characteristic lifetime.

We now turn our attention to the footpoint region of the simulated loop. Figure 5 shows an enlarged view of the C VII population at the left-hand footpoint. For the first minute or so of the simulation we see, as expected, that the C VII population remains constant. However, after 300 s there is a somewhat surprising increase in the amount of C VII present in the footpoint region. This increase becomes even more dramatic after 600 s.

At 300 s the temperature in the footpoint region at $s = 3 \times 10^8$ cm is on the order of 0.4 MK. Once again we may estimate the characteristic lifetime of C VII under these conditions. The recombination rate corresponding to C VII at this temperature is 2.3464×10^{-12} cm^3 s^{-1} and the footpoint number density is on the order of 10^{10} cm^{-3}. Therefore, the lifetime is approximately 40 s.

Before 300 s its lifetime should be somewhat longer than this (though still not as long as 300 s) because the recombination rate and the density are smaller. After 300 s the lifetime of C VII is expected to be much shorter because both the recombination rate and the density increase. However, contrary to this expectation, the amount of C VII actually increases as shown at 300 s and at 600 s.

The question naturally arises: how does the population of C VII persist so far beyond its characteristic lifetime?

The answer to this question lies in the flows that develop in the cooling loop (Fig. 4). We have already seen that the population of C VII persists for a long while in the upper regions of the loop, giving the flows sufficient time to develop and to carry a significant amount of C VII into the lower regions of the loop.

At 600 s the downflows are just about on the order of 10^6 cm s^{-1} (10 km s^{-1}) and have therefore been able to transport material (including the persistent C VII population) from higher up over distances on the order of 1000 km. At 1000 s the flows are even stronger and the population of C VII at the footpoints is correspondingly greater.

At 1500 s there is a significant reduction in the population of C VII in the footpoint regions. Figure 4 shows that the flows have also decreased in the footpoint regions and so less material is being brought in. Consequently, at 1500 s the flows are unable to replenish the C VII population by bringing in the C VII ions that have persisted for a long time in the upper atmosphere, before recombination appreciably depletes the footpoint population of C VII.

Though the flows have decreased at 1500 s, material is still being brought into the footpoint regions, thus increasing the density and consequently the radiative energy loss. The resulting greater rate of cooling also helps to reduce the C VII population.

Finally, we present the total emissivity profiles for the cooling loop calculated by summing the emission from all 15 elements included in the radiation model. Figures 6 and 7 show the total emissivity profiles for the identical simulation carried out assuming the ion population radiates in equilibrium (discussed at the beginning of this section). Recall that this loop cooled to its termination condition approximately 10 min faster (in loop evolution time) than the full nonequilibrium simulation. Figures 8 and 9 show the total emissivity profiles for the nonequilibrium simulation.

The reason for the difference in cooling time between the two simulations is immediately obvious from Figs. 6 and 8. For the first 300 s or so there are no major differences in magnitude between the equilibrium and nonequilibrium emissivity curves in the upper regions of the loop, suggesting that the dominant emitters (such as the ions of Fe) remain approximately in equilibrium. We confirm this expectation in Sect. 5. As the upper regions of the loop cool to transition region temperatures, the dominant transition region ions take over and these can be relatively long-lived (Mg IX, for example). Additionally, as plasma drains from the upper regions of the loop and the density in those regions decreases, the characteristic lifetimes of the ions increase. Therefore, by taking these considerations into account, the nonequilibrium calculation will eventually show an overabundance of relatively highly charged ions, which radiate more and more weakly as the plasma cools. This is precisely what we see in Figs. 6 and 8 after about 600 s. The nonequilibrium emissivity curve decreases in the upper regions of the loop in comparison with the equilibrium emissivity curve, reaching a factor of 3 and more difference after 1000 s. Consequently, the loop radiating in equilibrium cools significantly more quickly.

Figures 7 and 9 show an enlarged view of the equilibrium and nonequilibrium emissivities, respectively, in the left-most footpoint region. In this region we see a significant difference between the emissivity curves after only 300 s, which increases at subsequent times. There are two main reasons for these differences. Firstly, the emission from this region is dominated by transition region ions. These can be relatively long-lived (as above) and their populations can be shifted away from equilibrium very quickly at the densities under consideration. Secondly, the downflows make a contribution to the nonequilibrium ion populations by bringing a significant number of highly charged ions across a steep gradient into a region of markedly different plasma properties (as already discussed). The consequence of both of these considerations is a population of ions emitting in a region of much lower temperature than they would otherwise be found and the resulting decrease in emissivity shown at 300, 600 and 1000 s in Fig. 9 as compared with Fig. 7. This is significant because most of the radiation from a solar loop is emitted by the transition region.

These results emphasise the importance of accounting for the effects of a nonequilibrium ion population in radiation calculations when modelling the solar atmosphere.

5. Conclusions

We have performed a hydrodynamic simulation of a coronal loop, cooling from a peak temperature of about 1.5 MK to a peak temperature on the order of 0.3 MK, on a fixed, nonuniform grid. We have solved the fully time-dependent and

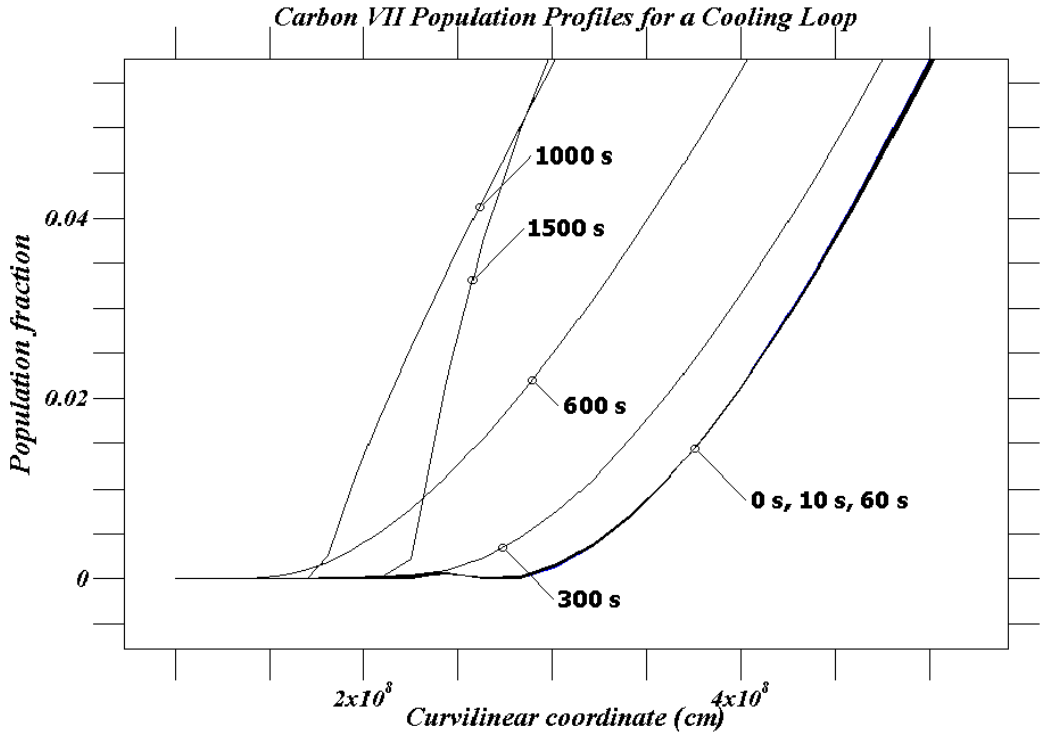

Fig. 5. An enlarged footpoint time series of C VII profiles.

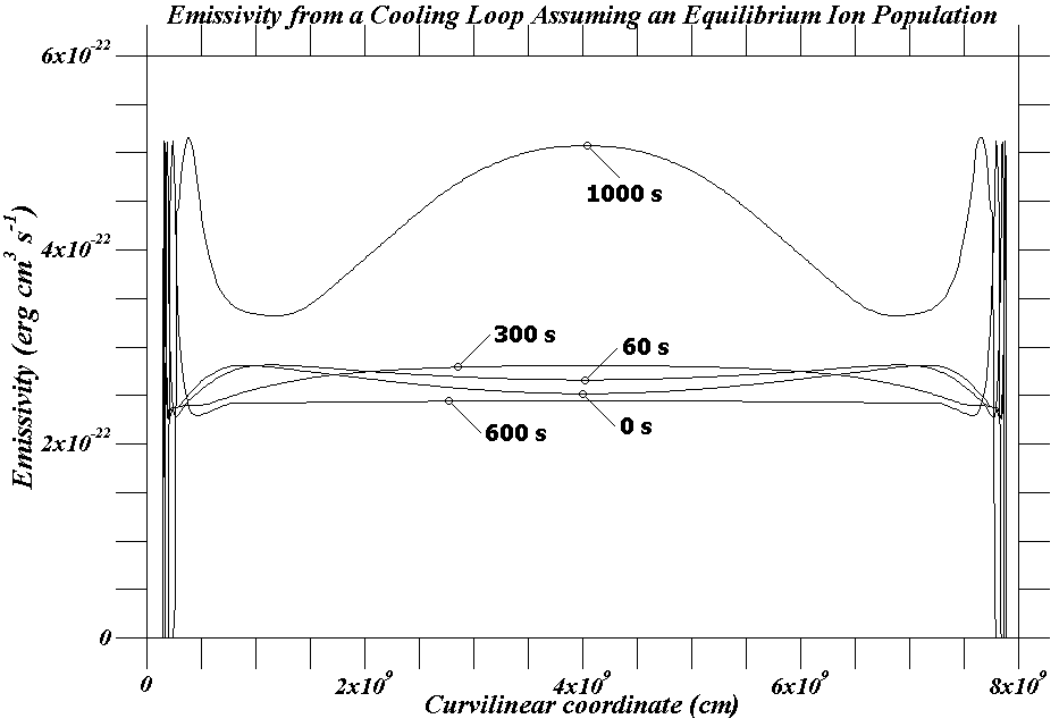

Fig. 6. A time series of total emissivity calculated assuming equilibrium ion populations in the cooling loop.

advective ion balance equation for each ion of the 15 most abundant elements of the solar atmosphere and have coupled these calculations to the hydrodynamics in order to perform a self-consistent calculation of the radiative energy loss at each time-step of the simulation. To the best of our knowledge, this is the first time that such a calculation has been performed for the conditions encountered in the solar atmosphere.

In the current paper we have only presented the response of the C VII ion population, however, we are easily able to repeat our analysis for any choice of ion(s) and a more detailed study including several important coronal and transition region ions will be the focus of a subsequent paper.

Clearly, significant departures from equilibrium can occur in a coronal ion population. An extremely important question

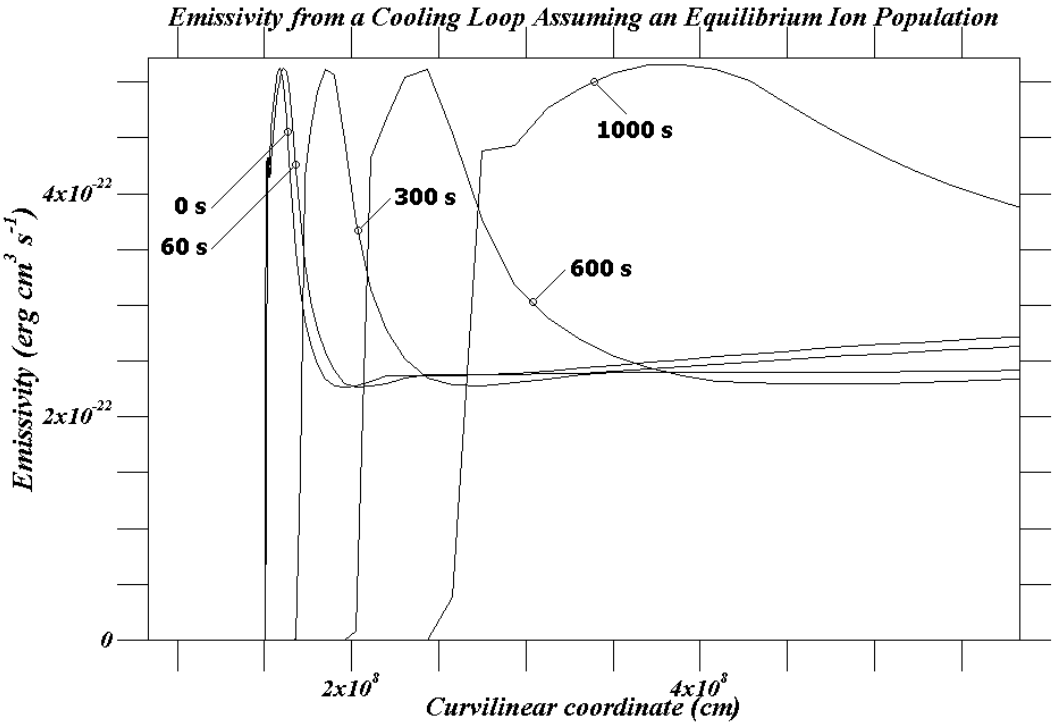

Fig. 7. An enlarged footpoint time series of total emissivity calculated assuming equilibrium ion populations.

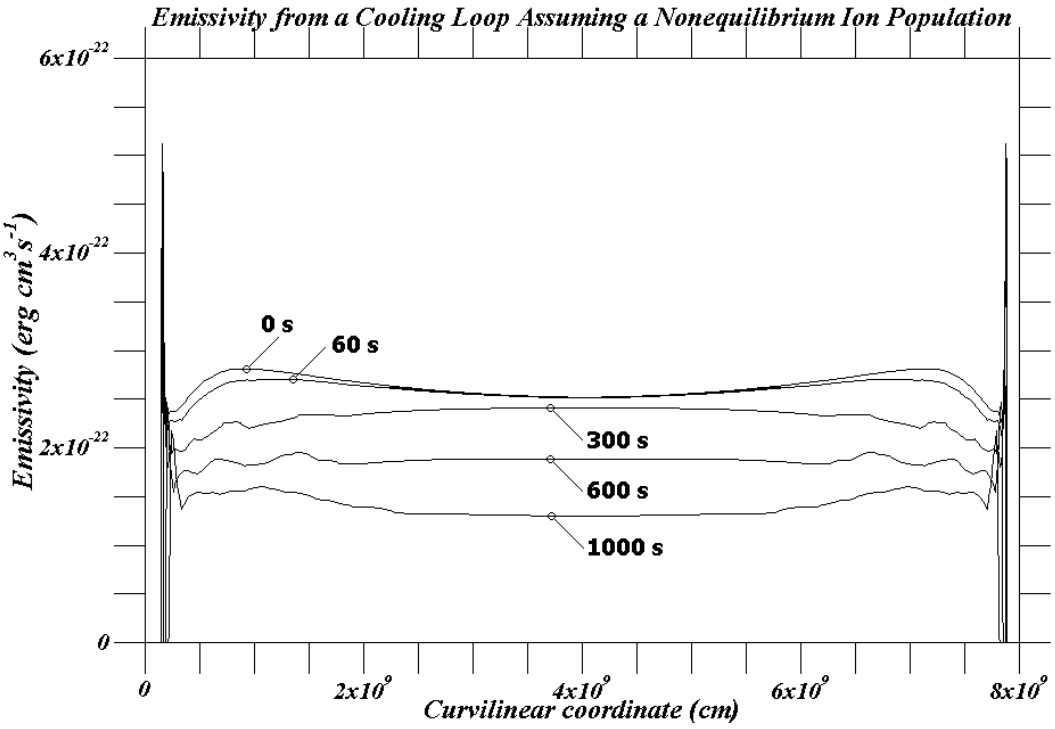

Fig. 8. A time series of total emissivity accounting for an ion population shifted away from equilibrium in the cooling loop.

is whether this holds true for the strongly radiating coronal ions, such as Fe IX and X (TRACE 171 Å). Taking Fe X at 1 MK as an example: the total ionisation and recombination rate is 2.2644×10^{-10} cm^3 s^{-1} (Mazzotta et al. 1998) and so in a plasma of $n = 10^8$ cm^{-3} the expected lifetime of Fe X is approximately 45 s. Therefore, we may expect Fe X to depart from its equilibrium population if the characteristic time-scale of temperature change is somewhat less than 1 min in a rarefied loop plasma. Given that observing instruments such as the TRACE satellite rely heavily upon emission from this ion and have a temporal cadence on the order of 1 s, this may well have significant consequences for temperature measurements derived from TRACE. Additionally, there are many other strong emission lines from coronal elements whose ion

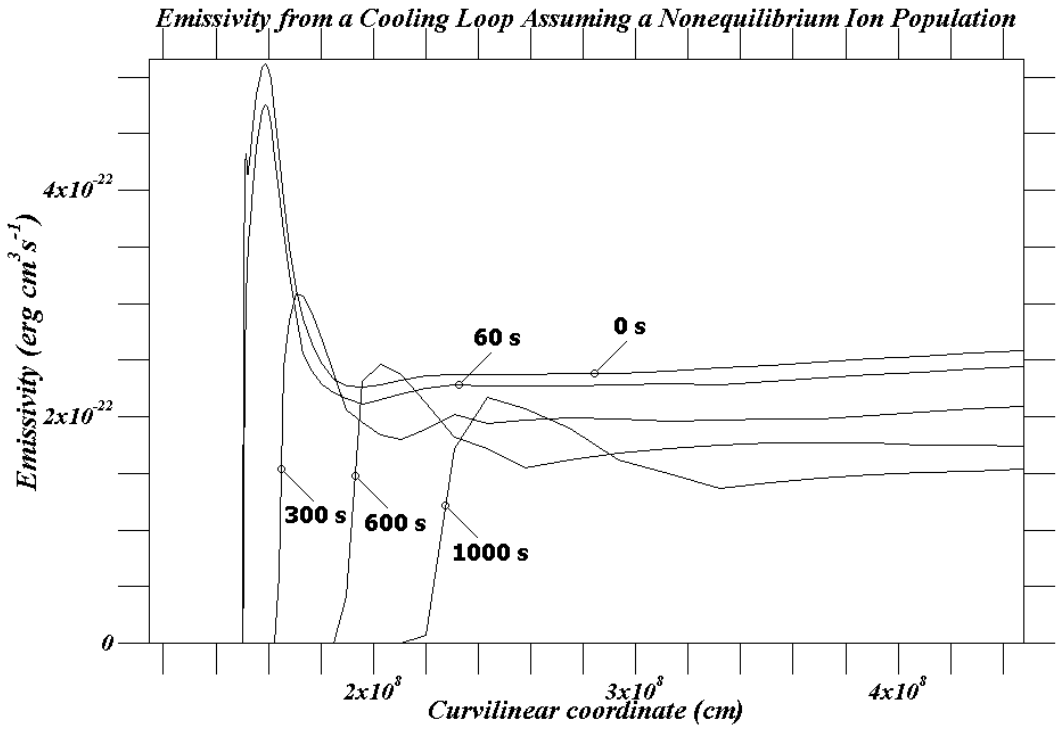

Fig. 9. An enlarged footpoint time series of total emissivity accounting for an ion population shifted away from equilibrium.

populations might well have considerably longer characteristic lifetimes in the rarefied coronal plasma.

There has recently been a substantial amount of interest in cooling coronal loops, though from considerably higher temperatures (~6 MK), with the intention of predicting what instruments such as CDS and TRACE might observe as the loops cool through their ranges of temperature sensitivity. It is likely that strong downflows observed by Doppler shifts in particular emission lines have a significant effect upon the observed temperature profiles of loops. Our future work will join these efforts and we hope to investigate the possibility that nonequilibrium ion populations (arising due to the temperature changes and the strong flows) have an effect upon the emission spectrum of the solar atmosphere, thus potentially explaining the observed thermal broadening of various emission lines (Sarro et al. 1999).

Furthermore, there is also a problem in reconciling the observed persistence of these very hot loops with theoretical modelling. Warren et al. (2002) simulate a cooling loop and show that it would be observed in the TRACE 171 and 195 Å filters simultaneously for about 800 s. However, they also state that a previous analysis has suggested these loops can persist for hours (Lenz et al. 1999). Nonequilibrium radiation can potentially contribute towards resolving this problem. As we have seen in Sect. 4, the total radiative emission calculated away from conditions of equilibrium can potentially be considerably reduced and the loops themselves could therefore persist for much longer periods of time than previous theoretical work has indicated.

Further work with our coupled nonequilibrium radiation and hydrodynamic codes will investigate this effect upon the rate of cooling for hot loops such as these.

Acknowledgements. SJB would like to thank Drs. R. Erdélyi, P. R. Young, G. Del-Zanna, A. Burgess, P. J. MacNeice, R. W. Walsh, J. A. Klimchuk and S.K. Antiochos for their help and advice during the development of the hydrodynamic and radiation codes. SJB and HEM also acknowledge and thank PPARC for their support. We thank the referee for his careful reading of the manuscript and for his suggestions, which have undoubtedly produced a much improved paper.

References

Arnaud, M., & Rothenflug, R. 1985, A&AS, 60, 425
Aschwanden, M. J., Schrijver, C. J., & Alexander, D. 2001, ApJ, 550, 1036
Cargill, P. J., Mariska, J. T., & Antiochos, S. K. 1995, ApJ, 439, 1034
Centrella, J., & Wilson, J. R. 1984, ApJS, 54, 229
Dere, K. P., Landi, E., Mason, H. E., Monsignori Fossi, B. C., & Young, P. R. 1997, A&AS, 125, 149
Erdélyi, R., Sarro, L. M., & Doyle, J. G. 1998, Proc. Solar Jets and Coronal Plumes, ESA SP-421, 207
Erdélyi, R., & Sarro, L. M. 1999, Proc. 8th SOHO Workshop, ESA SP-446, 299
Feldman, U. 1992, Phys. Scr., 46, 202
Klimchuk, J. A., Antiochos, S. K., & Mariska, J. T. 1987, ApJ, 320, 409
Lenz, D. D., De Luca, E. E., Golub, L., Rosner, R., & Bookbinder, J. A. 1999, ApJ, 517, L155
MacNeice, P. J., McWhirter, R. W. P., Spicer, D. S., & Burgess, A. 1984, Sol. Phys., 90, 357
Mazzotta, P., Mazzitelli, G., Colafrancesco, S., & Vittorio, N. 1998, A&AS, 133, 403

Mendoza-Briceño, C. A., Erdélyi, R., Sigalotti, & L. Di. G. 2002, ApJ, 579, L49
Oran, E. S., & Boris, J. P. 2001, Numerical Simulation of Reactive Flow (Cambridge University Press), ISBN 0 521 58175 3
Parker, E. N. 1988, ApJ, 330, 474
Press, W. H., Teukolsky, S. A., Vetterling, W. T., & Flannery, B. P. 1995, Numerical Recipes in C (Cambridge University Press), ISBN 0 521 43108 5
Priest, E. R., Foley, C., Heyvaerts, J., et al. 1998, Nature, 393, 545
Reale, F., & Peres, G. 2000, ApJ, 528, L45
Sarro, L. M., Erdélyi, R., Doyle, J. G., & Pérez, M. E. 1999, A&A, 351, 721
Schmelz, J. T., Scopes, R. T., Cirtain, J. W., Winter, H. D., & Allen, J. D. 2001, ApJ, 556, 896
Spadaro, D., Lanza, A. F., Lanzafame, A. C., et al. 2002, Proc. SOHO 11 Symp., ESA SP-508, 331
Teriaca, L., Doyle, J. G., Erdélyi, R., & Sarro, L. M. 1999, A&A, 352, L99
Warren, H. P., Winebarger, A. R., & Hamilton, P. S. 2002, ApJ, 579, L41
Widing, K. G., & Feldman, U. 2001, ApJ, 555, 426
van Leer, B. 1977, J. Comp. Phys., 23, 276
Young, P. R., Del Zanna, G., Landi, E., et al. 2003, ApJS, 144, 135